atmosphere

MDPI

Article

Characteristics of Atmospheric Pollutants in Paddy and Dry Field Regions: Analyzing the Oxidative Potential of Biomass Burning

Myoungki Song [1], Minwook Kim [2], Sea-Ho Oh [1], Geun-Hye Yu [1], Seoyeong Choe [1], Hajeong Jeon [1], Dong-Hoon Ko [1], Chaehyeong Park [1] and Min-Suk Bae [1,*]

[1] Department of Environmental Engineering, Mokpo National University, Muan 58554, Republic of Korea; msong@mnu.ac.kr (M.S.); osh9119mnudk@mokpo.ac.kr (S.-H.O.); fanygh89@mnu.ac.kr (G.-H.Y.); S184221@365.mokpo.ac.kr (S.C.); S214210@365.mokpo.ac.kr (H.J.); ehdgns8011@mokpo.ac.kr (D.-H.K.); pch123421@mokpo.ac.kr (C.P.)

[2] Climate Change Assessment Division, National Institute of Agricultural Sciences, Wanju 55365, Republic of Korea; minuk09@korea.kr

* Correspondence: minsbae@mnu.ac.kr; Tel.: +82-61-450-2485

Abstract: This study aimed to identify the characteristics of atmospheric pollutants emitted by agricultural activities and to evaluate factors that may cause harm to human health. For the research, atmospheric pollutants were measured over the course of a year in representative rice farming and field crop farming areas in South Korea. The results confirmed that the characteristics of atmospheric pollutants in agricultural areas are influenced by the nature of agricultural activities. Specifically, when comparing rice paddies and field crop areas, during summer, the correlation between oxidative potential and levoglucosan—a marker for biomass burning—weakens due to less burning activity in the rice-growing season, leading to lower oxidative potential despite different $PM_{2.5}$ across areas. The study also finds that methyl sulfonic acid, indicating marine influence, plays a big role in keeping oxidative potential low in summer. This suggests that the main causes of $PM_{2.5}$-related health risks in the area are from biomass burning and external sources, with burning being a significant factor in increasing oxidative potential. Based on these results, it is hoped that measures can be taken in the future to reduce atmospheric pollutants in agricultural areas.

Keywords: agricultural particulate matter; DTT-OP; levoglucosan; dithiothreitol

check for updates

Citation: Song, M.; Kim, M.; Oh, S.-H.; Yu, G.-H.; Choe, S.; Jeon, H.; Ko, D.-H.; Park, C.; Bae, M.-S. Characteristics of Atmospheric Pollutants in Paddy and Dry Field Regions: Analyzing the Oxidative Potential of Biomass Burning. *Atmosphere* **2024**, *15*, 493. https://doi.org/10.3390/atmos15040493

Academic Editor: Jin-Seok Han

Received: 18 March 2024
Revised: 10 April 2024
Accepted: 14 April 2024
Published: 17 April 2024

1. Introduction

Atmospheric pollutants can be emitted by various natural activities, but anthropogenic activities are considered the main cause of the increase in atmospheric pollutants [1]. The rise in atmospheric pollutants can adversely affect human health, a well-known fact evidenced by the increase in respiratory diseases and deaths due to the rise in particulate matter [2,3]. Thus, the increase in atmospheric pollutants is recognized as a significant social factor that can reduce human life expectancy and cause various economic losses [4]. For these reasons, efforts to reduce atmospheric pollutants are deemed essential in modern society, particularly the reduction of pollutants stemming from anthropogenic activities.

Recent studies have identified agricultural activities as a significant contributor to atmospheric pollution [4], attributed to the substantial volume of pollutants emitted by agriculture and their potential harm to human health [5,6]. Agricultural emissions include not only particulate matter but also various precursor gases necessary for the formation of $PM_{2.5}$. Previous research presented that agricultural activities are among the largest sources of particulate matter emissions across Europe. In China, 92.2% of NH_3 emissions come from agriculture, along with the production of various volatile organic compounds (VOCs) [7–9]. From a human health perspective, $PM_{2.5}$ (particulate matter with a diameter of less than 2.5 µm) emitted by agricultural activities is known to be harmful even at very low concentrations, with agriculture being a significant factor in deaths attributed to atmospheric pollutants in

Europe, Russia, the United States, Japan, and Canada [10–13]. Controlling pollutants from agricultural activities could potentially reduce a fifth of the global deaths caused by $PM_{2.5}$ [5]. To mitigate the $PM_{2.5}$ emitted by agricultural activities, it is necessary to first examine the characteristics of these emissions. However, the emission characteristics of $PM_{2.5}$ from agricultural activities can vary even for the same crops, depending on local soil characteristics, water conditions, cropping systems, and differences in agricultural practices [14–16]. Therefore, to understand the characteristics of $PM_{2.5}$ emitted from agricultural activities, it is crucial to consider variables such as soil characteristics, cropping systems, climate, and agricultural practices on a regional basis. However, accounting for all variables for each region, crop type, land characteristics, and agricultural activity is realistically impossible. This is why current studies on the emission characteristics of atmospheric pollutants from agricultural activities rely on bottom-up tracing methods based on field observations, necessitating observations of atmospheric pollutants specific to different crops and agricultural characteristics [14,17,18].

This research was conducted to identify the characteristics of $PM_{2.5}$ emitted by agricultural activities. Representative rice and field crop farming areas in South Korea were selected for observation over a year. Based on the observations, the study presents the characteristics of $PM_{2.5}$ emissions related to rice and field crop activities and identifies factors of oxidative potential from agricultural-area pollutants. The results are expected to serve as data for future studies on the emission characteristics of atmospheric pollutants from agricultural activities and to be utilized for managing pollutants emitted by such activities.

2. Materials and Methods

2.1. Measurement Locations and Sampling Period

The observation of atmospheric pollutants in agricultural areas was conducted in farmlands located in Buan (35°46′21″ N 126°40′05″ E) and Gochang (35°20′58″ N 126°35′50″ E), South Korea (Figure 1). The observation sites in Buan and Gochang are distinguished as rice and field crop farmlands, respectively, and are agricultural areas with no residential buildings or industrial complexes within a 1 km radius of the observation points. However, residential areas are located approximately 1.5 km away, and the sea is within 5 km to the west. The measurement period spanned one year, from 1 September 2022 to 31 August 2023, with atmospheric pollutants being observed from the 1st to the 24th of each month for quartz and Teflon filter sampling for 48 h. The time following the observation period each month was allocated for analysis and maintenance of the collection devices.

In order to compare the characteristics of the soil and cultivated crops in the study areas of Buan and Gochang, an examination was conducted. The soil in the Buan area is composed of approximately 74% loamy sand (46%) and sandy loam (24%), with specific soil textures including 19.45% sand, 31% loamy, and 21% silty loam. In contrast, the Gochang area exhibits a deeper effective soil depth with 0–20 cm at 15%, 20–50 cm at 15%, 50–100 cm at 28%, and over 100 cm at 34%, and the soil texture comprises 61% sandy clay loam, 9% sandy loam, and 7% loamy sand (Republic of Korea Land Information, Soil Portal: http://soil.rda.go.kr/soil/chart/chartSoilType.jsp accessed on 10 March 2024). Regarding the primary agricultural crops, the Buan region predominantly engages in paddy farming, with rice and rice barley accounting for approximately 85% of all cultivated crops. Meanwhile, Gochang's agricultural activities are more varied, with paddy farming representing about 12% of the total agricultural activities and field farming accounting for 85% (Buan County Office: https://www.buan.go.kr accessed on 10 March 2024). Specifically, the field crops in the Gochang area include watermelons (32%), cabbages (13%), radishes (19%), and onions (12%), totaling 22 different types of field crops (Gochang County Office: https://www.gochang.go.kr accessed on 10 March 2024). Additionally, both regions engage in orchard operations, albeit at a minimal level (<2%) compared to paddy and field farming activities. Given that the observational sites in Buan and Gochang are approximately 60 km apart, it is presumed that there are no significant differences in agricultural activities attributable to climate variations. The distinctions in agricultural practices are primarily due to the differences between paddy and field farming and the varying planting and harvesting times of the crops. Notably, South Korea experiences four distinct seasons, with paddy farming in the Buan area involving planting in April, followed by harvesting in September to October. In contrast, Gochang's cultivation cycles vary depending on the crop, with watermelons planted in April to May and harvested in June to August, onions planted in January to March and harvested in May to June, and radishes planted in August to September and harvested in November to December. Therefore, while the Buan area maintains a consistent planting and harvesting schedule, the Gochang area exhibits diversity in agricultural activities, conducting 2 or 3 farming operations annually based on the characteristics of the cultivated crops.

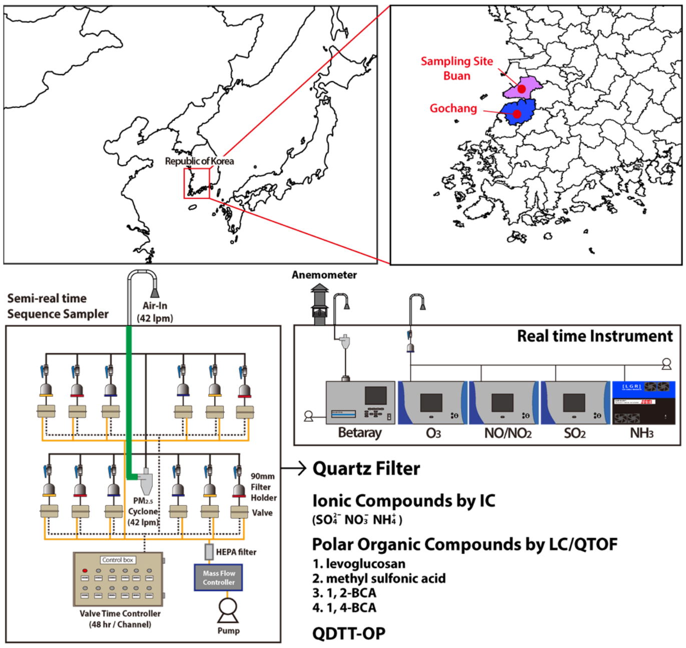

Figure 1. The observation of atmospheric pollutants in agricultural areas was conducted in farmlands located in Buan (35°46′21″ N 126°40′05″ E) and Gochang (35°20′58″ N 126°35′50″ E), South Korea.

2.2. Real-Time Measurements

Real-time measurements included the concentrations of PM_{10} and $PM_{2.5}$, as well as gaseous compounds such as NH_3, NO, NO_2, and O_3. PM_{10} and $PM_{2.5}$ were observed using a beta-ray measurement device (Spirant BAM 1020, Met One Instruments Inc., Grants Pass, OR, USA). Gaseous substances were measured in real-time using equipment for NH3 (cavity ring-down spectroscopy, CRDS G2013), NO and NO_2 (Serinus® 40, Ecotech ACOEM Group, Melbourne, Australia), SO_2 (Serinus® 50, Ecotech ACOEM Group, Melbourne, Australia), and O_3 (Serinus® 10, Ecotech ACOEM Group, Melbourne, Australia). All equipment for measuring gaseous compounds was calibrated using a three-point calibration before measurement. After calibration, a different concentration was injected to ensure measurements were within 5% of the target concentration.

2.3. Chemical Speciation

Sample collection for $PM_{2.5}$ was conducted at 48-h intervals. Specifically, $PM_{2.5}$ collection was performed at a flow rate of 42.0 L/min onto a 90 mm quartz filter, allowing for the acquisition of 12 samples on a monthly basis. Analyzed components of $PM_{2.5}$ included organic carbon (OC), elemental carbon (EC) and water-soluble ionic components (NH_4^+, NO_3^-, SO_4^{2-}, Cl^-, Na^+, and K^+). In addition, collected $PM_{2.5}$ samples were analyzed for organic molecular markers such as levoglucosan, 1,2-benzenecarboxylic acid (1,2-BCA), 1,4-benzenecarboxylic acid (1,4-BCA), and methanesulfonic acid (MSA), and a hazard evaluation was performed using the quinone dithiothreitol-based oxidative potential (QDTT-OP) analysis method.

OC and EC were analyzed using a carbon analyzer (Lab-based OCEC Carbon Aerosol Analyzer, Sunset Laboratory Inc., Tigard, OR, USA), based on the National Institute of Occupational Safety & Health (NIOSH 5040) protocol. Water-soluble ions were quantitatively analyzed using ion chromatography for anions (Metrohm 930 Switzerland, Metrosep A Supp 150/4.0 column, 3.7 mM Na_2CO_3 & 1.0 mM $NaHCO_3$) and cations (Metrohm 930 Switzerland, Metrosep C4-250/4.0 column, 5 mM HNO_3) after thermostatic extraction for 2 h using an ultrasonic cleaner (8800, Branson, St. Louis, MO, USA) connected to a thermostatic circulator (CA-111, Eyela, Tokyo, Japan) with the sectioned collection filter and 10 mL of distilled water. Organic marker substances such as levoglucosan, 1,2-BCA, 1,4-BCA, and MSA were analyzed using an LC-QToF (LC: Agilent Infinity II, QToF: SCIEX X500r) after extraction with a water and methanol 1:1 solution using an SB-C18 column (Agilent Poroshell 120, Santa Clara, CA, USA).

The QDTT-OP experimental method was determined by normalizing to quinone. Briefly, the redox reaction-based DTT-OP method is performed by reacting $PM_{2.5}$ chemical components with DTT, utilizing the rate of DTT reduction induced by various chemical components in $PM_{2.5}$, including reactive oxygen species (ROS) [19,20]. However, the DTT reduction rate in the DTT-OP method can vary depending on the initial DTT concentration used in the analysis, making it challenging to quantitatively assess human health risks using DTT-OP [21]. The QDTT-OP method, an improvement over the traditional DTT-OP, normalizes the DTT reduction rate based on the concentration of 9,10-Phenanthrenequinone and then evaluates the DTT reduction rate of $PM_{2.5}$ samples [22]. The experiment involved injecting 0.2 mM DTT, 2.41 mM 5,5-dithio-bis (2-nitrobenzoic acid) (DTNB), and 500 mM potassium phosphate monobasic into the $PM_{2.5}$ extract solution and adjusting the pH to 7.4, followed by the addition of 100 mM potassium phosphate dibasic. The mixture was then processed using a dispenser (Multiflo FX, Multi-Mode Dispenser, Agilent Technologies, Santa Clara, CA, USA) and reacted under 37 °C, with constant stirring. The absorbance at 412 nm was measured four times over 40 min to assess TNB. Every 15 samples were reanalyzed, and quinone samples were injected to maintain analysis accuracy and precision within 5%.

2.4. SOR, NOR, and NHR

The calculated values for the Sulfate Oxidation Ratio (SOR), Nitrate Oxidation Ratio (NOR), and Nitrogen Homologation Ratio (NHR) utilized the analyzed water-soluble ions NH_4^+, NO_3^-, and SO_4^{2-}, along with observed gaseous results for NOx, SO_2, and NH_3. SOR, NOR, and NHR are defined as the molar ratios of SO_4^{2-}, NO_3^-, and NH_4^+ to the total oxidized and reduced forms of sulfur (S) and nitrogen (N), respectively [23,24]. The NOR, SOR, and NHR were calculated using the formulas below.

$$\mathrm{NOR} = [NO_3^-]/([NO_x] + [NO_3^-]) \quad (1)$$

$$\mathrm{SOR} = [SO_4^{2-}]/([SO_2] + [SO_4^{2-}]) \quad (2)$$

$$\mathrm{NHR} = [NH_4^+]/([NH_3] + [NH_4^+]) \quad (3)$$

3. Results and Discussions

3.1. Characteristics of Atmospheric Pollutants in Agricultural Areas

The results of the chemical analysis in Buan by paddy fields, and Gochang by dry fields, are presented in Table 1. As shown in the table, the temperature and humidity in both Buan and Gochang were similar, averaging 14 ± 10 °C and 78 ± 10% RH, respectively. The concentrations of gaseous compounds such as NO, NO_2, SO_2, and O_3 were found to be at levels where no significant differences could be attributed, with concentrations of approximately 1.5 ppb for NO, 4.3 ppb for NO_2, 2 ppb for SO_2, and 33 ppb for O_3, respectively. However, the concentration of NH_3 was significantly different, with about 23 ppb in Buan and 30 ppb in Gochang, indicating that the ammonia levels in the dry farming region were over 30% higher than in the paddy farming region. This difference is presumed to be due to variations in the amounts of fertilizers and compost used in crop cultivation, as well as the timing of biomass-burning activities between paddy and dry field agriculture. Generally, the primary nutrients required for crop growth include N, P, and K, with fertilizers and composts mainly containing these elements [25]. N, in particular, is released into the atmosphere as NH_3 following application to the soil, influenced by temperature and evaporation processes [26]. Fertilizer application in agricultural practices occurs primarily during soil tilling before seeding and in large quantities immediately after seeding, followed by intermittent applications (https://www.nongsaro.go.kr accessed on 10 March 2024; Rural Development Administration, Wanju, Republic of Korea). Thus, the timing of fertilizer and compost application is concentrated around the soil-tilling and seeding periods, correlating with higher atmospheric concentrations of NH_3. Furthermore, the emission sources of NH_3 in agricultural areas include not only the use of fertilizers and composts but also the burning of agricultural residues after harvest [27]. Buan, being an area that exclusively cultivates rice in paddy fields, has a single crop cultivation cycle annually, whereas Gochang cultivates a variety of crops, such as watermelons, chili peppers, and radishes, sequentially throughout the year. Therefore, the timing of fertilizer application and the burning of agricultural residues in Buan is less frequent compared to Gochang, where these activities occur more regularly prior to the cultivation of each crop and after the harvest. Consequently, compared to the paddy farming region of Buan, the dry farming region of Gochang has higher frequencies of fertilizer and compost use and agricultural residue burning, leading to higher concentrations of atmospheric NH_3.

Table 1. Summary statistics of average concentrations of measured species in rice field areas of Buan and in Gochang areas of Jeollabuk-do during the measurement period.

Compound	Unit	Buan	Gochang
Temperature	Celsius	14.04 ± 10.00	14.14 ± 10.00
Humidity	%	78.70 ± 8.81	77.43 ± 9.57
NH_3	ppb	23.18 ± 11.08	30.18 ± 11.57
NO	ppb	1.48 ± 0.71	1.62 ± 0.50
NO_2	ppb	4.46 ± 2.58	4.12 ± 1.99
SO_2	ppb	2.80 ± 0.97	1.34 ± 0.59
O_3	ppb	34.65 ± 10.94	32.98 ± 9.03
PM_{10}	μg/m^3	39.41 ± 23.21	34.57 ± 23.48
$PM_{2.5}$	μg/m^3	22.47 ± 12.24	15.97 ± 9.78
OC	μg/m^3	4.23 ± 2.46	3.80 ± 2.12
EC	μg/m^3	0.41 ± 0.22	0.42 ± 0.21
Cl^-	μg/m^3	0.23 ± 0.27	0.28 ± 0.26
NO_3^-	μg/m^3	4.05 ± 5.97	3.81 ± 5.51
SO_4^{2-}	μg/m^3	3.27 ± 1.89	3.05 ± 1.82
Na^+	μg/m^3	0.07 ± 0.06	0.01 ± 0.10
NH_4^+	μg/m^3	2.57 ± 1.93	2.53 ± 1.84
K^+	μg/m^3	0.13 ± 0.13	0.12 ± 0.11
Levoglucosan	μg/m^3	0.042 ± 0.044	0.057 ± 0.070
1,2-BCA [1)]	μg/m^3	0.004 ± 0.003	0.005 ± 0.003
1,4-BCA [2)]	μg/m^3	0.015 ± 0.013	0.016 ± 0.011
MSA [3)]	μg/m^3	0.029 ± 0.020	0.023 ± 0.016
QDTT-OP	μM/m^3	0.130 ± 0.061	0.121 ± 0.057
NHR	-	0.098 ± 0.048	0.077 ± 0.039
NOR	-	0.207 ± 0.174	0.205 ± 0.173
SOR	-	0.419 ± 0.148	0.594 ± 0.181
$[NH_4^+]/[SO_4^{2-}]$	-	4.53 ± 3.20	4.67 ± 2.23
$[NO_3^-]/[SO_4^{2-}]$	-	1.98 ± 2.69	1.83 ± 1.91

[1)] 1,2-benzenecarboxylic acid; [2)] 1,4-benzenecarboxylic acid; [3)] methanesulfonic acid.

The difference in characteristics between single-crop paddy farming regions and multi-crop dry farming regions is also evident in the ratio of PM_{10} and $PM_{2.5}$ concentrations. PM emissions from agricultural activities are categorized into particles arising from mechanical factors, such as soil-cultivation, crop-harvesting, and grain-handling processes, and secondary precursor emissions from the use of compost and pesticides [14,28–30]. Particles from mechanical factors tend to be larger, with mineral matter as the primary component and soil dust as the main cause [31–33]. Thus, PM_{10} in agricultural activities is primarily generated from dust raised by soil cultivation and other mechanical factors, while $PM_{2.5}$ is more influenced by secondary precursors, such as compost and pesticides. Since $PM_{2.5}$ is inhalable and smaller in size, it is considered more dangerous for human health compared to PM_{10}, which is merely respirable.

The ratios of $PM_{10}/PM_{2.5}$ in Buan and Gochang were 1.73 and 2.14, respectively, with Buan showing seasonal ratios of 2.26 in spring, 1.63 in summer, 1.50 in fall, and 1.53 in winter, and Gochang showing 2.42 in spring, 2.27 in summer, 2.25 in fall, and 1.62 in winter. This indicates that Buan experiences an increase in the $PM_{10}/PM_{2.5}$ ratio during the spring due to soil-tilling activities in paddy farming but does not show a continuous increase. In contrast, Gochang demonstrates a persistent increase in the $PM_{10}/PM_{2.5}$ ratio following spring, attributed to the sequential cultivation of different crops requiring soil tilling for each, resulting in a continuous increase in PM_{10}.

The study examined the concentration of $PM_{2.5}$ and its compositional components in the research area. The average concentration of $PM_{2.5}$ was 22.47 $\mu g/m^3$ in Buan and 15.97 $\mu g/m^3$ in Gochang, indicating that the paddy farming region of Buan had higher $PM_{2.5}$ concentrations compared to the dry farming region of Gochang. An analysis of the $PM_{2.5}$ components in Buan showed that approximately 20.65% were composed of carbonaceous material (OC and EC), with soluble ions accounting for about 45.93%. In Gochang, carbonaceous components comprised 26.42%, and soluble ions comprised 61.37% of $PM_{2.5}$. Therefore, over 60% of $PM_{2.5}$ in both agricultural regions was identified as being composed of carbonaceous material and soluble ions, highlighting the significant contribution of these components to agricultural-area $PM_{2.5}$. However, the paddy farming region of Buan had a combined carbonaceous and soluble ion content of approximately 66.58%, compared to 87.79% in the dry farming region of Gochang. This difference is presumed to be influenced by the emission of biogenic volatile organic compounds (BVOCs) such as isoprene and monoterpenes from rice cultivation areas. These components, based on their high reactivity, contribute to the formation of secondary organic aerosols (SOAs) and O_3, with previous studies indicating the emission of monoterpenes from areas cultivating rice [34–36]. The observation results from Buan and Gochang indicated that the OC/EC ratio, used to estimate the SOC ratio, was 10.32 in Buan and 9.05 in Gochang, showing a higher SOC ratio in Buan. In addition, the O_3 concentrations during spring and summer, when BVOCs are predominantly emitted, were 44 ppb in Buan and 41 ppb in Gochang during spring, and 37 ppb in Buan and 33 ppb in Gochang during summer, indicating differences. Comparing PM_{10} and $PM_{2.5}$ concentrations, as shown in Table 1, Buan had higher PM_{10} concentrations, i.e., 39.41 $\mu g/m^3$, compared to 34.57 $\mu g/m^3$ in Gochang, a difference of approximately 14%. Conversely, the difference in $PM_{2.5}$ concentrations was significantly higher in Buan than in Gochang by about 41%, indicating a higher generation of secondary particles in Buan compared to Gochang.

The soluble ions that make up $PM_{2.5}$ were analyzed, focusing on NO_3^-, SO_4^{2-}, NH_4^+, Cl^-, Na^+, and K^+. Among these, NO_3^-, SO_4^{2-}, and NH_4^+, (known as SNA), which are secondary inorganic aerosols, accounted for 97% of the analyzed soluble ions in both Buan and Gochang. Thus, a majority of soluble ions were confirmed to be from SNA, indicating a significant influence of SNA on $PM_{2.5}$ mass. The research evaluated the formation characteristics of secondary inorganic aerosols (SIAs) based on SNA, examining ammonium-rich conditions and ratios of NHR, NOR, and SOR. The ammonium-rich conditions, assessed using the molar ratio of $[NH_4^+]/[SO_4^{2-}]$, suggest an environment conducive to SIA formation through SNA if the ratio is above 1.5, and less conducive (ammonium-poor) if below 1.5 [23,30,37]. The molar ratio of $[NO_3^-]/[SO_4^{2-}]$ was also evaluated, with a higher ratio indicating a greater contribution of NO_3^- to SIA formation due to the sequential neutralization reactions of atmospheric NH_3 with SOx products followed by NOx products [30,38,39]. The $[NH_4^+]/[SO_4^{2-}]$ ratio was 4.53 in Buan and 4.67 in Gochang, with $[NO_3^-]/[SO_4^{2-}]$ ratios of 1.98 in Buan and 1.83 in Gochang. Therefore, both regions, irrespective of paddy or dry field characteristics, were evaluated as ammonium-rich, indicating an environment conducive to SIA formation through SNA, with NO_3^- contributing significantly to SIA formation compared to SO_4^{2-}. In addition, NH_3 concentrations at the observation points were more than tenfold higher than those measured in the capital of South Korea from 2015 to 2017 (2.26 ppb) [40], indicating particle formation from abundant atmospheric NH_3 in an ammonium-rich environment. The correlation between gaseous SO_2, NO_2, and SO_4^{2-} and NO_3^- in $PM_{2.5}$ was also examined. The results showed a correlation coefficient (r^2) between SO_2 and SO_4^{2-} of 0.008 in Buan and 0.002 in Gochang, and between NO_2 and NO_3^- of 0.601 in Buan and 0.537 in Gochang. These results suggest that SO_4^{2-} in $PM_{2.5}$ could be influenced rather than local SO_2 emissions, while NO_3^- in $PM_{2.5}$ is generated from local NOx emissions.

To further investigate the correlation between gaseous precursors (NH_3, NOx, and SO_2) and secondary inorganic aerosol particles, the formation rates of secondary inorganic aerosol particles were calculated. NHR, NOR, and SOR represent the degree of oxidation and reduction when atmospheric NH_3, NOx, and SO_2 form particulate matter. Higher values of NHR, NOR, and SOR indicate active oxidation and reduction processes, generating more secondary inorganic aerosol particles in the atmosphere. Typically, when NHR, NOR, and SOR are below 0.1, primary emission sources dominate, and values above 0.1 indicate chemically induced generation [41–43]. The calculated seasonal results for NHR, NOR, and SOR in the research area are presented in Figure 2. NHR averaged 0.098 in Buan and 0.077 in Gochang, indicating more active chemical reactions of gaseous precursors in Buan compared to Gochang. Seasonally, both Buan and Gochang exhibited NHR values above 0.1 during winter, suggesting more active chemical reactions in winter compared to other seasons. Typically, SNA's SIA reactions, driven by photochemical reactions, would result in higher NHR values in summer compared to winter. However, the study found the lowest NHR values in summer (0.074 in Buan; 0.052 in Gochang) and the highest in winter. This discrepancy may be attributed to the interaction between atmospheric NH_3 and NOx. Nitrate formed from the reaction of NH_3 and NOx is relatively stable at low temperatures and unstable at high temperatures [44,45], making the conversion of atmospheric NOx into particulate nitrate more challenging during summer. Indeed, the concentration of NO_3^- in $PM_{2.5}$ averaged 4.05 $\mu g/m^3$ in Buan and 3.81 $\mu g/m^3$ in Gochang, but in summer, NO_3^- concentrations were 0.26 $\mu g/m^3$ in Buan and 0.42 $\mu g/m^3$ in Gochang, indicating lower nitrate formation during summer. Additionally, based on the correlation between $[NO_3^-]/[SO_4^{2-}]$ and gaseous SO_2 and NO_2 with SO_4^{2-} and NO_3^-, the research area was confirmed to have stronger local reactions of NO_3^- in SIA formation compared to SO_4^{2-}. Therefore, the higher NHR in winter compared to summer is likely influenced by temperature-dependent nitrate formation.

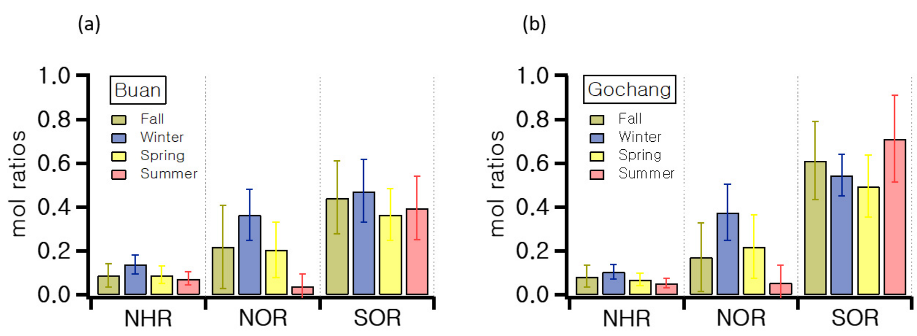

Figure 2. Seasonal average results of NHR, NOR, and SOR for $PM_{2.5}$ in rice field areas of Buan and Gochang in Jeollabuk-do, Republic of Korea. (**a**) Buan (**b**) Gochang.

Examining NOR in the research area, we found that Buan had average values of 0.205 in spring, 0.040 in summer, 0.219 in fall, and 0.364 in winter, averaging 0.207, while Gochang had 0.219 in spring, 0.055 in summer, 0.171 in fall, and 0.375 in winter, averaging 0.205. Thus, NOR indicated predominance of chemically generated particles except in summer, where lower results were likely influenced by temperature effects hindering nitrate formation. SOR in Buan was 0.366 in spring, 0.396 in summer, 0.443 in fall, and 0.472 in winter, averaging 0.419, while Gochang had 0.494 in spring, 0.711 in summer, 0.612 in fall, and 0.546 in winter, averaging 0.594. This shows that both Buan and Gochang exhibited efficient photochemical reactions of gaseous precursors, with Gochang displaying a wider seasonal variance. Our seasonal examination of SOR revealed winter as the highest season in Buan, contrary to summer in Gochang. Various factors may contribute, but the influence of biomass-burning emissions from agricultural activities is considered significant. Biomass burning is a major source of SO_2 emissions in agricultural areas, with some regions reporting an 80–90% contribution to SO_2 emissions from biomass burning [46,47]. Biomass burning typically occurs after crop harvest and before soil tilling in Buan, a paddy farming region, primarily in autumn and winter, whereas Gochang, with its sequential cultivation of various crops, experiences biomass burning not only in autumn and winter but also in spring and summer. Therefore, SOR in Buan peaks during autumn and winter with active biomass burning, while Gochang sees a summer peak due to both biomass burning and the most active photochemical reactions. In additional, as previously mentioned, the correlation between atmospheric SO_2 concentrations and SO_4^{2-} was found to be very low in the research area, suggesting that SOR is likely generated from widespread SOx undergoing atmospheric chemical reactions during regional transport.

3.2. Assessment of Health Hazard Factors in $PM_{2.5}$ from Agricultural Areas

To identify the oxidative potential in $PM_{2.5}$ collected from the study area that could potentially induce human health hazards, an analysis using the QDTT-OP method was conducted. The results revealed that, in the Buan area, the concentrations of QDTT-OP were 0.145 $\mu M/m^3$ in spring, 0.072 $\mu M/m^3$ in summer, 0.132 $\mu M/m^3$ in autumn, and 0.172 $\mu M/m^3$ in winter, with an average of 0.130 $\mu M/m^3$. In the Gochang area, the concentrations were 0.144 $\mu M/m^3$ in spring, 0.075 $\mu M/m^3$ in summer, 0.164 $\mu M/m^3$ in autumn, and 0.100 $\mu M/m^3$ in winter, averaging 0.121 $\mu M/m^3$. When evaluating the hazard based solely on QDTT-OP concentrations, both Buan and Gochang areas exhibited higher levels during winter and spring compared to summer and autumn.

To determine the $PM_{2.5}$ components affecting QDTT-OP, a daily time-series analysis, as depicted in Figure 3, was performed to correlate QDTT-OP with $PM_{2.5}$ concentration and its constituents, including OC, EC, and soluble ions. The analysis confirmed a correlation between QDTT-OP and the concentrations of $PM_{2.5}$, OC, EC, and soluble ions. Specifically, when examining the correlation between QDTT-OP and analyzed components based on the r^2, $PM_{2.5}$ showed a correlation of 0.69 in Buan and 0.67 in Gochang. For OC, the correlation was 0.67 in Buan and 0.55 in Gochang; for EC, 0.51 in Buan and 0.65 in Gochang; and for soluble ions, 0.66 in Buan and 0.53 in Gochang. However, a closer examination of autumn and winter, the seasons with the highest QDTT-OP concentrations, revealed that QDTT-OP had the strongest correlation with OC (Buan $r^2 > 0.90$, Gochang $r^2 > 0.89$). This indicates that, while the human health hazard assessed based on QDTT-OP is not independent of $PM_{2.5}$ concentrations and soluble ions, the high QDTT-OP concentrations are relatively more influenced by OC.

To further investigate OC as the influencer of high concentrations of QDTT-OP in Buan and Gochang, a detailed analysis of OC components was conducted. This analysis aimed to infer the sources impacting human health hazards based on the content of OC. The organic components identified within OC were levoglucosan, 1,2-BCA, 1,4-BCA, and MSA. Levoglucosan, a substance produced exclusively through the decomposition of cellulose and hemicellulose at combustion temperatures above 300 °C, serves as a representative marker of biomass burning. Meanwhile, 1,2-BCA and 1,4-BCA are recognized as water-soluble organic acids involved extensively in various atmospheric chemical processes and serve as molecular markers. MSA is utilized as an indicator for secondary production influenced by precursors such as SO_2, associated with long-range transport related to marine influences [28,48,49]. The results for identifying the components affecting QDTT-OP, as shown in Table 2, revealed seasonal concentration variations. As indicated in Table 2, QDTT-OP concentrations were affected by variations in OC concentrations, with a significant correlation found with levoglucosan. To examine this relationship more closely, the correlation between QDTT-OP, OC, and levoglucosan was analyzed, yielding the results presented in Figure 4. As demonstrated in Figure 4, QDTT-OP was correlated with OC throughout the research period, and the correlation with levoglucosan increased during spring and winter when QDTT-OP concentrations were high. Considering that levoglucosan is an indicator of biomass burning and that biomass burning in agricultural areas primarily occurs after crop harvest and before soil tilling in winter and spring, it can be inferred that the source of high QDTT-OP concentrations is biomass burning. Thus, it is evident that the source of increased human health hazards in $PM_{2.5}$ from agricultural areas is attributed to emissions from biomass burning.

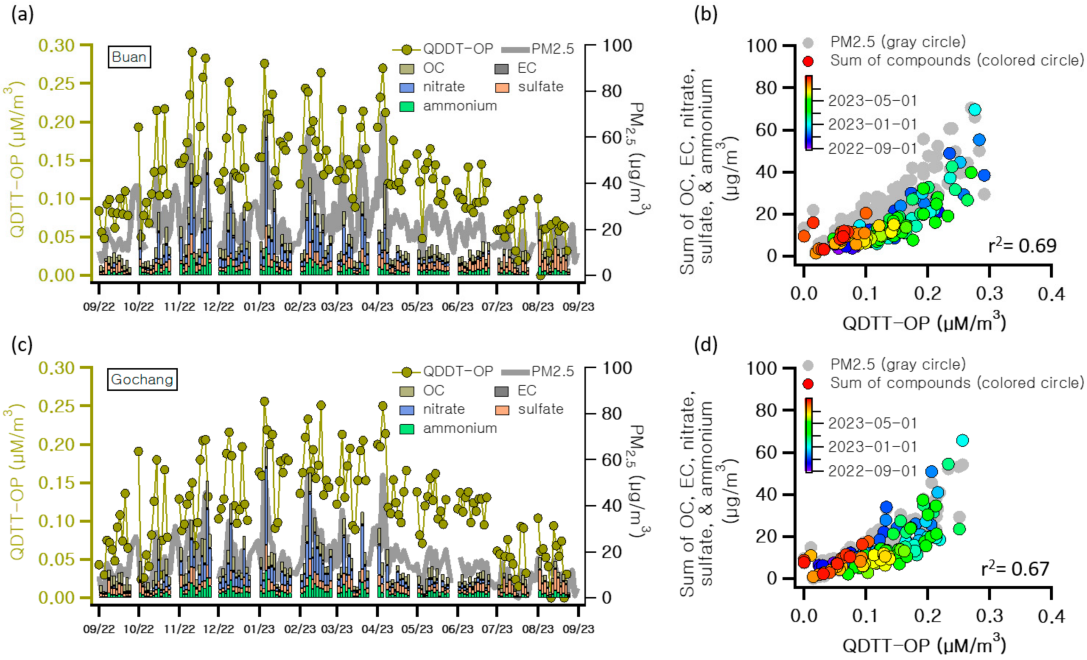

Figure 3. Forty-eight-hour averaged time series results of organic carbon (OC), elemental carbon (EC), sulfate, nitrate, and ammonium, along with a scatter plot between the sum of sulfate, nitrate, and ammonium and QDTT-OP in rice field areas of Buan and Gochang in Jeollabuk-do, Republic of Korea. (**a**,**b**) Buan (**c**,**d**) Gochang.

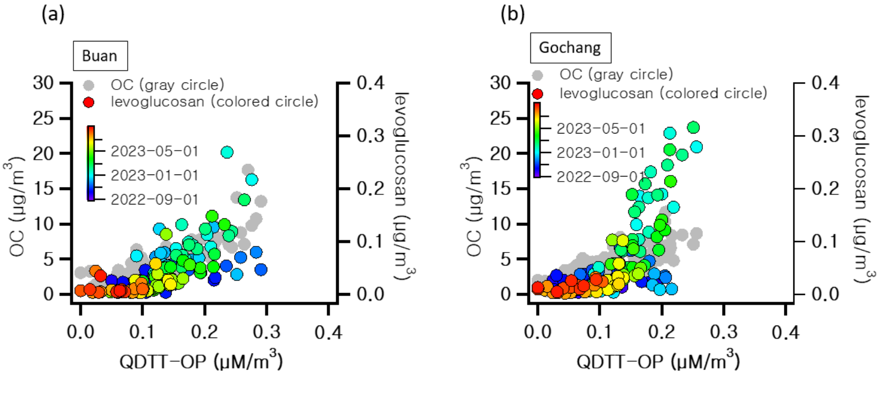

Figure 4. Correlation of QDTT-OP with organic carbon (OC) and levoglucosan. (**a**) Buan (**b**) Gochang.

Table 2. $PM_{2.5}$ composition in rice field areas of Buan and Gochang in Jeollabuk-do by season.

Compound Unit		QDTT μM/m³	OC μg/m³	EC μg/m³	LEVOG μg/m³	1,2-BCA μg/m³	1,4-BCA μg/m³	MSA μg/m³
Fall	Buan	0.132 ±0.066	4.645 ±2.726	0.288 ±0.141	0.029 ±0.022	0.005 ±0.002	0.018 ±0.015	0.025 ±0.01
	Gochang	0.100 ±0.053	4.871 ±2.544	0.35 ±0.162	0.029 ±0.02	0.005 ±0.002	0.015 ±0.011	0.022 ±0.009
Winter	Buan	0.172 ±0.047	5.14 ±2.402	0.542 ±0.232	0.091 ±0.05	0.005 ±0.002	0.023 ±0.015	0.02 ±0.01
	Gochang	0.164 ±0.045	4.36 ±1.997	0.514 ±0.263	0.115 ±0.096	0.006 ±0.003	0.020 ±0.012	0.014 ±0.008
Spring	Buan	0.145 ±0.045	4.392 ±2.708	0.517 ±0.222	0.037 ±0.035	0.004 ±0.003	0.012 ±0.007	0.037 ±0.025
	Gochang	0.144 ±0.043	3.65 ±1.702	0.519 ±0.193	0.066 ±0.062	0.005 ±0.003	0.018 ±0.01	0.032 ±0.023
Summer	Buan	0.072 ±0.034	2.75 ±0.984	0.305 ±0.102	0.012 ±0.012	0.001 ±0.001	0.006 ±0.004	0.035 ±0.026
	Gochang	0.075 ±0.041	2.272 ±1.013	0.308 ±0.118	0.018 ±0.018	0.002 ±0.002	0.011 ±0.008	0.023 ±0.014

Meanwhile, during summer, when QDTT-OP concentrations were lower, as illustrated in Figure 4, the correlation with levoglucosan appeared relatively diminished. Considering the rice cultivation period in Buan, we see that the summer season corresponds to the growth phase of rice, during which biomass-burning activities are virtually nonexistent. Indeed, as Table 2 indicates, the concentration of levoglucosan during summer was the lowest compared to autumn, winter, and spring, suggesting minimal biomass-burning activities during this time. In additional, as shown in Figure 3, QDTT-OP demonstrates a strong correlation with $PM_{2.5}$ concentration (r^2 > 0.67). However, despite significant differences in $PM_{2.5}$ concentrations between Buan (14.67 μg/m^3) and Gochang (8.75 μg/m^3) during summer, the QDTT-OP concentrations remained similar at 0.072 μM/m^3 and 0.075 μM/m^3, respectively. This result implies the existence of a common source persistently causing low QDTT-OP concentrations, aside from biomass-burning sources that induce high concentrations of QDTT-OP.

To identify the components affecting QDTT-OP during the summer, when the influence of biomass-burning emissions is minimal, an investigation was conducted, leading to the findings presented in Figure 5. As Figure 5 demonstrates, the low QDTT-OP concentrations in summer were correlated with MSA, with an r^2 of 0.43 or higher (0.43 in Buan and 0.45 in Gochang), indicating a relation between summer QDTT-OP concentrations and MSA. Considering MSA as an indicator for long-range transport related to marine influences, its role in affecting the generation of secondary products from precursors such as SO_2, and the previously mentioned correlation between $SO_4{}^{2-}$ and external SO_2 inputs, it can be inferred that the research area, being adjacent to the western coast of South Korea, is influenced by long-range marine influx. It can be concluded that the low QDTT-OP concentrations in the study area are influenced by long-range transport related to marine impacts. In essence, the research identifies two main sources of substances inducing human health hazards in $PM_{2.5}$ from the study area: external influx components and biomass-burning emissions, with high concentrations of QDTT-OP significantly increased by biomass burning. Although the current research does not encompass all elements affecting the human health hazards of $PM_{2.5}$ in the study area, it clearly indicates the influence of both biomass-burning sources and long-range marine influx components on human health hazards.

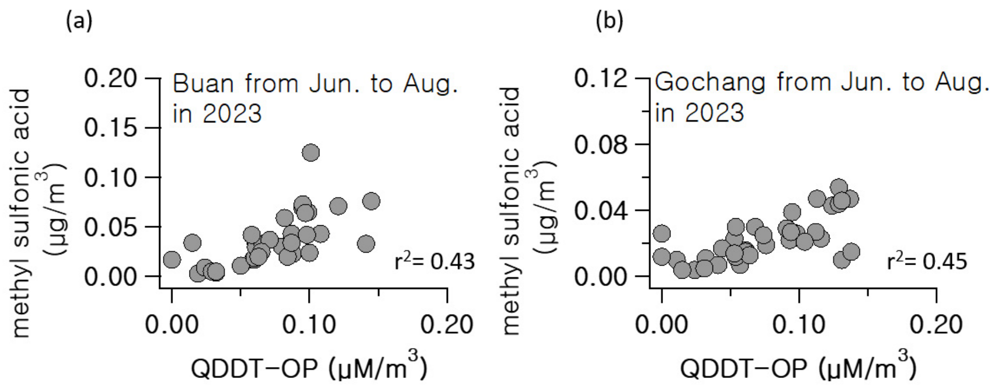

Figure 5. Correlation of QDTT-OP with methanesulfonic acid (MSA). (**a**) Buan (**b**) Gochang.

4. Conclusions

This study aimed to examine the characteristics of air pollutants in agricultural areas, focusing on paddy and dry field farming regions, and to estimate the sources of human health hazards in these agricultural settings. During the summer, the correlation between QDTT-OP and levoglucosan significantly drops, reflecting minimal biomass burning due to the rice cultivation period in Buan. This period sees the lowest levoglucosan, indicating reduced biomass-burning activities and, consequently, lower QDTT-OP, despite varying $PM_{2.5}$ between locations. The study identifies MSA as a key influencer of low QDTT-OP concentrations during summer, suggesting long-range transport from marine sources as a significant factor. This finding points to two primary sources of $PM_{2.5}$ human health hazards in the area: biomass-burning emissions and external influx components, with biomass burning predominantly raising QDTT-OP concentrations. The results of this research imply two significant insights. First, understanding the characteristics of air pollutants emitted due to differences in paddy and dry farming activities allows for the prediction of air pollutant emissions based on the timing of agricultural activities and the characteristics of cultivated crops. Second, from a human health hazard perspective, the study provides a basis for managing hazardous emissions sources, such as biomass burning. It is hoped that the outcomes of this research will the enable effective management of air pollutants emitted from agricultural areas in the future.

Author Contributions: M.S. and M.K. contributed to this work by completing the experiment measurements, data analysis, and manuscript preparation. S.-H.O., G.-H.Y., S.C., H.J., D.-H.K. and C.P. contributed to research sample analyses. M.-S.B. contributed to the experimental planning and data analysis. All authors have read and agreed to the published version of the manuscript.

Funding: This study was supported by the Cooperative Research Program for Agriculture Science & Technology Development (RS-2022-RD010226) Rural Development Administration, Republic of Korea. This work was supported by a grant from the National Institute of Environmental Research (NIER), funded by the Ministry of Environment (MOE) of the Republic of Korea (NIER-2021-03-03-007).

Institutional Review Board Statement: Not applicable.

Informed Consent Statement: Not applicable.

Data Availability Statement: The data presented in this study are available on request from the corresponding author. The data are not publicly available due to data policy of the National Institute of Agricultural Sciences, Republic of Korea.

Conflicts of Interest: The authors declare no conflict of interest.

References

1. Kampa, M.; Castanas, E. Human health effects of air pollution. *Environ. Pollut.* **2008**, *151*, 362–367. [CrossRef] [PubMed]
2. Dominici, F.; Peng, R.D.; Bell, M.L.; Pham, L.; McDermott, A.; Zeger, S.L.; Samet, J.M. Fine particulate air pollution and hospital admission for cardiovascular and respiratory diseases. *JAMA* **2006**, *295*, 1127–1134. [CrossRef] [PubMed]

3. Yang, S.J.; Liu, X.; Bi, Y.; Ning, S.; Qiao, Q.; Yu, Q.; Zhang, J. Risks related to heavy metal pollution in urban construction dust fall of fast-developing Chinese cities. *Ecotoxicol. Environ. Saf.* **2020**, *197*, 110628. [CrossRef] [PubMed]
4. Sekar, M.; Kumar, T.R.P.; Kumar, M.S.G.; Vaníčková, R.; Maroušek, J. Techno-economic review on short-term anthropogenic emissions of air pollutants and particulate matter. *Fuel* **2021**, *305*, 121544. [CrossRef]
5. Cox, L.A. Re-assessing human mortality risks attributed to $PM_{2.5}$-mediated effects of agricultural ammonia. *Environ. Res.* **2023**, *223*, 115311. [CrossRef] [PubMed]
6. Pozzer, A.; Tsimpidi, A.P.; Karydis, V.A.; de Meij, A.; Lelieveld, J. Impact of agricultural emission reductions on fine-particulate matter and public health. *Atmos. Chem. Phys.* **2017**, *17*, 12813–12826. [CrossRef]
7. Li, R.; Chen, W.; Xiu, A.; Zhao, H.; Zhang, X.; Zhang, S.; Tong, D.Q. A comprehensive inventory of agricultural atmospheric particulate matters (PM_{10} and $PM_{2.5}$) and gaseous pollutants (VOCs, SO_2, NH_3, CO, NOx and HC) emissions in China. *Ecol. Indic.* **2019**, *107*, 105609. [CrossRef]
8. Li, M.; Zhang, Q.; Kurokawa, J.-I.; Woo, J.-H.; He, K.; Lu, Z.; Carmichael, G.R. MIX: A mosaic Asian anthropogenic emission inventory under the international collaboration framework of the MICS-Asia and HTAP. *Atmos. Chem. Phys.* **2017**, *17*, 935–963. [CrossRef]
9. Mozaffar, A.; Zhang, Y.-L. Atmospheric Volatile Organic Compounds (VOCs) in China: A Review. *Curr. Pollut. Rep.* **2020**, *6*, 250–263. [CrossRef]
10. Bauer, S.E.; Tsigaridis, K.; Miller, R. Significant atmospheric aerosol pollution caused by world food cultivation. *Geophys. Res. Lett.* **2016**, *43*, 5394–5400. [CrossRef]
11. Pinault, L.; Tjepkema, M.; Crouse, D.L.; Weichenthal, S.; van Donkelaar, A.; Martin, R.V.; Burnett, R.T. Risk estimates of mortality attributed to low concentrations of ambient fine particulate matter in the Canadian community health survey cohort. *Environ. Health* **2016**, *15*, 18. [CrossRef] [PubMed]
12. Shi, L.; Zanobetti, A.; Kloog, I.; Coull, B.A.; Koutrakis, P.; Melly, S.J.; Schwartz, J.D. Low-concentration $PM_{2.5}$ and mortality: Estimating acute and chronic effects in a population-based study. *Environ. Health Perspect.* **2016**, *124*, 46–52. [CrossRef] [PubMed]
13. Lee, C.J.; Martin, R.V.; Henze, D.K.; Brauer, M.; Cohen, A.; van Donkelaar, A. Response of global particulate-matter-related mortality to changes in local precursor emissions. *Environ. Sci. Technol.* **2015**, *49*, 4335–4344. [CrossRef] [PubMed]
14. Chen, W.; Tong, D.Q.; Zhang, S.; Zhang, X.; Zhao, H. Local PM_{10} and $PM_{2.5}$ emission inventories from agricultural tillage and harvest in northeastern China. *J. Environ. Sci.* **2017**, *57*, 15–23. [CrossRef] [PubMed]
15. Nelson, A.J.; Koloutsou-Vakakis, S.; Rood, M.J.; Myles, L.; Lehmann, C.; Bernacchi, C.; Lin, J. Season-long ammonia flux measurements above fertilized corn in central Illinois, USA, using relaxed eddy accumulation. *Agric. For. Meteorol.* **2017**, *239*, 202–212. [CrossRef]
16. Wang, H.; Yilihamu, Q.; Yuan, M.; Bai, H.; Xu, H.; Wu, J. Prediction models of soil heavy metal(loid)s concentration for agricultural land in Dongli: A comparison of regression and random forest. *Ecol. Indic.* **2020**, *119*, 106801. [CrossRef]
17. Recio, J.; Montoya, M.; Ginés, C.; Sanz-Cobena, A.; Vallejo, A.; Alvarez, J.M. Joint mitigation of NH_3 and N_2O emissions by using two synthetic inhibitors in an irrigated cropping soil. *Geoderma* **2020**, *373*, 114423. [CrossRef]
18. Sanz-Cobena, A.; Lassaletta, L.; Estellés, F.; Del Prado, A.; Guardia, G.; Abalos, D.; Billen, G. Yield-scaled mitigation of ammonia emission from N fertilization: The Spanish case. *Environ. Res. Lett.* **2014**, *9*, 125005. [CrossRef]
19. Gao, D.; Mulholland, J.A.; Russell, A.G.; Weber, R.J. Characterization of water-insoluble oxidative potential of $PM_{2.5}$ using the dithiothreitol assay. *Atmos. Environ.* **2020**, *224*, 117327. [CrossRef]
20. Li, Q.; Wyatt, A.; Kamens, R.M. Oxidant generation and toxicity enhancement of aged-diesel exhaust. *Atmos. Environ.* **2009**, *43*, 1037–1042. [CrossRef]
21. Lin, M.; Yu, J.Z. Dithiothreitol (DTT) concentration effect and its implications on the applicability of DTT assay to evaluate the oxidative potential of atmospheric aerosol samples. *Environ. Pollut.* **2019**, *251*, 938–944. [CrossRef] [PubMed]
22. Song, M.-K.; Choi, J.; Oh, S.-H.; Choe, S.; Yu, G.-H.; Cho, S.-S.; Park, J.; Bae, M.-S. Diurnal dithiothreitol assays for biomass burning source in $PM_{1.0}$ and $PM_{2.5}$ during summer and winter. *Atmos. Environ.* **2023**, *313*, 120033. [CrossRef]
23. Hu, G.; Zhang, Y.; Sun, J.; Zhang, L.; Shen, X.; Lin, W.; Yang, Y. Variability, formation and acidity of water-soluble ions in $PM_{2.5}$ in Beijing based on the semi-continuous observations. *Atmos. Res.* **2014**, *145*, 1–11. [CrossRef]
24. Meng, Z.; Xu, X.; Lin, W.; Ge, B.; Xie, Y.; Song, B.; Jia, S.; Zhang, R.; Peng, W.; Wang, Y.; et al. Role of ambient ammonia in particulate ammonium formation at a rural site in the North China Plain. *Atmos. Chem. Phys.* **2018**, *18*, 167–184. [CrossRef]
25. Wang, H.; Wu, L.; Wang, X.; Zhang, S.; Cheng, M.; Feng, H.; Fan, J.; Zhang, F.; Xiang, Y. Optimization of water and fertilizer management improves yield, water, nitrogen, phosphorus and potassium uptake and use efficiency of cotton under drip fertigation. *Agric. Water Manag.* **2021**, *245*, 106662. [CrossRef]
26. Bouwman, A.; Boumans, L.; Batjes, N. Estimation of global NH_3 volatilization loss from synthetic fertilizers and animal manure applied to arable lands and grasslands. *Glob. Biogeochem. Cycles* **2002**, *16*, 8-1–8-14. [CrossRef]
27. Bray, C.D.; Battye, W.H.; Aneja, V.P.; Schlesinger, W.H. Global emissions of NH_3, NOx, and N_2O from biomass burning and the impact of climate change. *J. Air Waste Manag. Assoc.* **2021**, *71*, 102–114. [CrossRef]
28. Achad, M.; Caumo, S.; de Castro Vasconcellos, P.; Bajano, H.; Gómez, D.; Smichowsk, P. Chemical markers of biomass burning: Determination of levoglucosan, and potassium in size-classified atmospheric aerosols collected in Buenos Aires, Argentina by different analytical techniques. *Microchem. J.* **2018**, *139*, 181–187. [CrossRef]

29. Pattey, E.; Qiu, G. Trends in primary particulate matter emissions from Canadian agriculture. *J. Air Waste Manag. Assoc.* **2012**, *62*, 737–747. [CrossRef]
30. Song, M.; Kim, M.; Oh, S.-H.; Park, C.; Kim, M.; Kim, M.; Lee, H.; Choe, S.; Bae, M.-S. Influences of Organic Volatile Compounds on the Secondary Organic Carbon of Fine Particulate Matter in the Fruit Tree Area. *Appl. Sci.* **2021**, *11*, 8193. [CrossRef]
31. Clausnitzer, H.; Singer, M.J. Environmental influences on respirable dust production from agricultural operations in California. *Atmos. Environ.* **2000**, *34*, 1739–1745. [CrossRef]
32. Han, Q.; Wang, M.; Cao, J.; Gui, C.; Liu, Y.; He, X.; He, Y.; Liu, Y. Health risk assessment and bioaccessibilities of heavy metals for children in soil and dust from urban parks and schools of Jiaozuo, China. *Ecotoxicol. Environ. Saf.* **2020**, *191*, 110157. [CrossRef] [PubMed]
33. Qin, M.; Jin, Y.; Peng, T.; Zhao, B.; Hou, D. Heavy metal pollution in Mongolian-Manchurian grassland soil and effect of long-range dust transport by wind. *Environ. Int.* **2023**, *177*, 108019. [CrossRef] [PubMed]
34. Arneth, A.; Monson, R.K.; Schurgers, G.; Niinemets, Ü.; Palmer, P.I. Why are estimates of global terrestrial isoprene emissions so similar (and why is this not so for monoterpenes)? *Atmos. Chem. Phys.* **2008**, *8*, 4605–4620. [CrossRef]
35. Atkinson, R.; Arey, J. Gas-phase tropospheric chemistry of biogenic volatile organic compounds: A review. *Atmos. Environ.* **2003**, *37*, 197–219. [CrossRef]
36. Tani, A.; Sakami, T.; Yoshida, M.; Yonemura, S.; Ono, K. Emission of Terpenoid Compounds from Rice Plants. *Environments* **2023**, *10*, 49. [CrossRef]
37. Lin, Y.C.; Zhang, Y.L.; Fan, M.Y.; Bao, M. Heterogeneous formation of particulate nitrate under ammonium-rich regimes during the high-$PM_{2.5}$ events in Nanjing, China. *Atmos. Chem. Phys.* **2020**, *20*, 3999–4011. [CrossRef]
38. Xu, W.; Liu, X.; Liu, L.; Dore, A.J.; Tang, A.; Lu, L.; Zhang, F. Impact of emission controls on air quality in Beijing during APEC 2014: Implications from water-soluble ions and carbonaceous aerosol in $PM_{2.5}$ and their precursors. *Atmos. Environ.* **2019**, *210*, 241–252. [CrossRef]
39. Zhang, Y.; Lang, J.; Cheng, S.; Li, S.; Zhou, Y.; Chen, D.; Wang, H. Chemical composition and sources of PM_1 and $PM_{2.5}$ in Beijing in autumn. *Sci. Total Environ.* **2018**, *630*, 72–82. [CrossRef]
40. Shim, C.; Han, J.; Henze, D.K.; Shephard, M.W.; Zhu, L.; Moon, N.; Kharol, S.K.; Dammers, E.; Cady-Pereira, K. Impact of NH_3 Emissions on Particulate Matter Pollution in South Korea: A Case Study of the Seoul Metropolitan Area. *Atmosphere* **2022**, *13*, 1227. [CrossRef]
41. Sun, Y.; Zhuang, G.; Tang, A.; Wang, Y.; An, Z. Chemical characteristics of $PM_{2.5}$ and PM_{10} in haze-fog episodes in Beijing. *Environ. Sci. Technol.* **2006**, *40*, 3148–3155. [CrossRef] [PubMed]
42. Wang, H.; Wang, S.; Zhang, J.; Li, H. Characteristics of $PM_{2.5}$ Pollution with Comparative Analysis of O_3 in Autumn-Winter Seasons of Xingtai, China. *Atmosphere* **2021**, *12*, 569. [CrossRef]
43. Liang, Y.; Jiang, H.; Liu, X. Characteristics of atmospheric ammonia and its impacts on SNA formation in $PM_{2.5}$ of Nanchang, China. *Atmos. Pollut. Res.* **2024**, *15*, 102059. [CrossRef]
44. Chow, J.C.; Watson, J.G.; Lowenthal, D.H.; Magliano, K.L. Loss of $PM_{2.5}$ Nitrate from Filter Samples in Central California. *J. Air Waste Manag. Assoc.* **2005**, *55*, 1158–1168. [CrossRef] [PubMed]
45. Griffith, S.M.; Huang, X.H.H.; Louie, P.K.K.; Yu, J.Z. Characterizing the thermodynamic and chemical composition factors controlling $PM_{2.5}$ nitrate: Insights gained from two years of online measurements in Hong Kong. *Atmos. Environ.* **2015**, *122*, 864–875. [CrossRef]
46. Arndt, R.L.; Carmichael, G.R.; Streets, D.G.; Bhatti, N. Sulfur dioxide emissions and sectorial contributions to sulfur deposition in Asia. *Atmos. Environ.* **1997**, *31*, 1553–1572. [CrossRef]
47. Ren, Y.A.; Shen, G.; Shen, H.; Zhong, Q.; Xu, H.; Meng, W.; Zhang, W.; Yu, X.; Yun, X.; Luo, Y.; et al. Contributions of biomass burning to global and regional SO_2 emissions. *Atmos. Res.* **2021**, *260*, 105709. [CrossRef]
48. Bae, M.-S.; Schauer, J.J.; Turner, J.R. Estimation of the monthly average ratios of organic mass to organic carbon for fine particulate matter at an urban site. *Aerosol Sci. Technol.* **2006**, *40*, 1123–1139. [CrossRef]
49. Yu, Q.; Chen, J.; Qin, W.; Cheng, S.; Zhang, Y.; Ahmad, M.; Ouyang, W. Characteristics and secondary formation of water-soluble organic acids in PM_1, $PM_{2.5}$ and PM_{10} in Beijing during haze episodes. *Sci. Total Environ.* **2019**, *669*, 175–184. [CrossRef]